

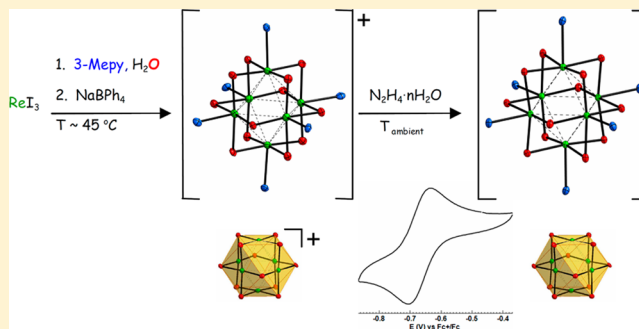
First Oxido-Bridged Cubo-Octahedral Hexanuclear Rhenium Clusters

Marta S. Krawczyk,* Monika K. Krawczyk, Miłosz Siczek, and Tadeusz Lis

Faculty of Chemistry, University of Wrocław, F. Joliot-Curie 14 Street, 50-383 Wrocław, Poland

Supporting Information

ABSTRACT: The first discrete hexanuclear metal clusters with cores adopting the $M_6(\mu-O)_{12}$ cubo-octahedral topology have been synthesized in the course of a simple one-pot reaction. We present a new class of rhenium clusters which are the first hexanuclear rhenium complexes with 12 bridging ligands and the first clusters with octahedrally arranged Re atoms bridged only by O atoms forming a unique cube-like $Re_6(\mu-O)_{12}$ unit. Our synthetic strategy demonstrates a new approach to the syntheses of polynuclear rhenium complexes under mild conditions. We discovered that the $[Re_6(\mu-O)_{12}(3-Mepy)_6]BPh_4$ cluster compound has the ability to undergo reversible or/and quasireversible redox reactions without changing spatial structure and overall geometry. Subsequently, a reduction reaction of $[Re_6(\mu-O)_{12}(3-Mepy)_6]BPh_4$ was performed successfully and almost quantitatively resulting in the formation of the molecular $[Re_6(\mu-O)_{12}(3-Mepy)_6]$ complex.



INTRODUCTION

The majority of transition metal hexanuclear complexes adopt two kinds of geometry: $M_6(\mu_3-L)_8$ (I), polyhedron composed of octahedrally arranged metal atoms bridged by eight μ_3 -ligands forming a cube, or $M_6(\mu-L)_{12}$ (II), M_6 -octahedron encapsulated by $\mu-L_{12}$ -cubo-octahedron. To date, there have been no reports of hexanuclear metal single-cluster species of the $M_6(\mu-O)_{12}$ cubo-octahedral geometry. Although Mo, W, and Nb form oxide anions and molecular complexes of the $M_6(\mu_6-O)(\mu-O)_{12}$ stoichiometry,¹ named Lindqvist hexametallates, the presence of O atom in the center of such polyhedron results in non-cubo-octahedral topology. Moreover, in the case of Mo, W, and Nb, polymeric oxide species are known where the discrete $M_6(\mu-O)_{12}$ units can be distinguished.²

Among polynuclear rhenium complexes, hexanuclear clusters have attracted considerable interest because of their application as building blocks for molecular and supramolecular design as well as for their electrochemical³ and photophysical properties⁴ and potential application in catalysis.⁵ Through extensive research on the hexanuclear rhenium clusters (denoted as Re_6), two kinds of geometry have been obtained so far. A significant majority of Re_6 complexes adopt the I geometry (Figure S1a, Supporting Information). This type of spatial structure is observed for clusters consisting of a core of the general formula $\{Re_6(\mu_3-Q)_{8-n}(\mu_3-X)_n\}^m$, where Q = S, Se, Te; X = Cl, Br; $n = \{0-4\}$, $m = \{2-6\}$, while an oxidation state of rhenium is predominantly +3 (configuration d^4).⁶⁻⁹ The analogous chalcogenide Re_6 compounds with one, two, or four μ_3 -O atoms in the structure adopt the same geometry as in I.¹⁰ Another kind of the geometry (III) is observed for complexes of a $[Re_6(\mu-Br)_6(\mu_3-Br)_2Br_6]^-$ stoichiometry,¹¹ where Re atoms are located in vertices of a trigonal prism (Figure S1b, Supporting Information).

A great majority of Re_6 complexes were obtained in high temperature, self-assembly reactions in sealed quartz vessels and predominantly in melts.⁷ Herein, we report a new class of rhenium complexes which establish a new kind of metal clusters and a novel approach to the syntheses of polynuclear rhenium compounds under mild conditions. To the best of our knowledge, our studies are unique toward the syntheses of the Re_6 complexes containing only the oxygen atoms as bridging ligands.

We discovered that, during the one-pot reaction in the presence of tertiary aromatic amines (L) and water, rhenium(III) halides can form the new kind of hexanuclear complexes of the unique $[Re_6(\mu-O)_{12}L_6]^+$ stoichiometry and the novel cube-like geometry (Figures 1 and 2).

RESULTS AND DISCUSSION

In the clusters reported here, 6 Re atoms are arranged octahedrally, and 12 O atoms are located over edges of Re_6 polyhedron as μ ligands. The formed composition is a Re_6 octahedron inscribed within a O_{12} -cubo-octahedron (Re–O–Re angles range between ca. 82° and 92°, Table 1). In other words, the O atoms linked by Re atoms form a frame of the polyhedron, which can be described as a cube without vertices. Each Re atom centers the cube face, while each O atom is located in the center of cube edge bonding two Re atoms (Figure 2b,c). The coordination sphere of each rhenium atom can be approximated by the square pyramid geometry, where O atoms (inner ligands) are located in vertices of square base and Re atom centers the base. The fifth coordination place of Re atom is occupied by a molecule of amine (L), apical ligand, while the sixth one is vacant and directed toward the cluster

Received: January 22, 2014

Published: June 13, 2014

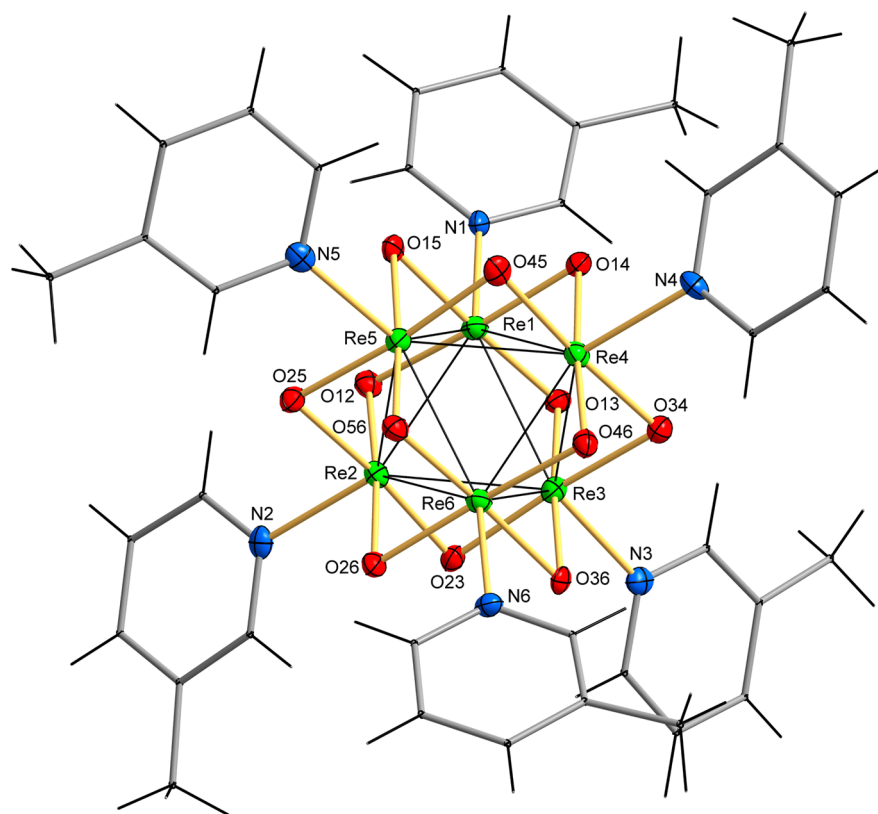


Figure 1. Overall geometry of the $[\text{Re}_6(\mu\text{-O})_{12}(\text{3-Mepy})_6]^+$ complex cation of C_1 symmetry (**1a**). The Re–Re bonds are shown with dark solid lines. Displacement ellipsoids of Re, O, and N atoms are shown at the 50% probability level. For clarity the 3-picoline rings with attached H atoms are shown in the wireframe representation.

center. The stoichiometry of studied clusters can be denoted as $M_6L^i_{12}L^a_6$ (i = inner, a = apical)¹² where $L^i = \text{O}$, $L^a = \text{amine}$.

Dodeca- μ -oxido-hexa(3-methylpyridine)-*octahedro*-hexarhenium-(12 Re–Re)(1+) tetraphenylborate, of the $[\text{Re}_6(\mu\text{-O})_{12}(\text{3-Mepy})_6]\text{BPh}_4$ (**1**) (3-Mepy = 3-picoline) formula (Figures 1 and 2a), was obtained in the reaction of rhenium(III) iodide with 3-methylpyridine and water under mild conditions (45–50 °C, under N_2). Subsequently, an isolated precipitate was treated by an excess of NaBPh_4 in acetonitrile giving the $[\text{Re}_6(\mu\text{-O})_{12}(\text{3-Mepy})_6]\text{BPh}_4$ (**1**) in the form of three kinds of crystals. The probable mechanism of formation of $\{\text{Re}_6(\mu\text{-O})_{12}\}^+$ clusters is apparent fragment condensation of the trinuclear species.⁷ In the course of the reaction the cleavage of Re–I bonds in the polymeric structure of ReI_3 ¹³ may occur releasing trinuclear $\text{Re}_3(\mu\text{-I})_3$ units, which undergo hydrolysis and apparent fragment condensation forming a hexanuclear oxidocomplex. Afterward, cyclic voltammetry experiments performed for **1** revealed that $[\text{Re}_6(\mu\text{-O})_{12}\text{L}_6]^+$ species can be reduced and oxidized reversibly or/and quasireversibly. The results of electrochemical studies prompted us to explore whether **1** might be reduced under chemical reaction. This was indeed accomplished by carrying out a reaction of **1** with hydrazine hydrate which resulted successfully in the formation of the one-electron reduced crystalline molecular $[\text{Re}_6(\mu\text{-O})_{12}(\text{3-Mepy})_6]\cdot 11\text{H}_2\text{O}$ (**2**) complex (dodeca- μ -oxido-hexa(3-methylpyridine)-*octahedro*-hexarhenium(12 Re–Re)—water (1/11)) of very similar spatial structure and overall geometry compared to **1**. All obtained crystals were characterized by the single-crystal X-ray diffraction;¹⁴ complexes **1** and **2** were studied by NMR, IR, FIR spectroscopy, and mass spectrometry, and magnetic measurements were performed. The X-ray studies revealed that, in **1**, based

upon the $[\text{Re}_6]^{25+}$ core, the formal oxidation state of rhenium atom is $+4^{1/6}$. The magnetic measurement proved that the studied complex is paramagnetic with one unpaired electron (Figure 3); the effective magnetic moment (μ_{eff}) equals $1.76 \mu_B$ per cluster. This result may suggest a delocalization of an unpaired electron onto the Re_6 unit, whereas in **2** the $[\text{Re}_6]^{24+}$ core occurs, which corresponds to +4 oxidation state (d^3 configuration) of each Re atom, affording a diamagnetic behavior. Therefore, we expected a smaller distortion of the Re_6 polyhedron in **2** from the O_h symmetry (or nearly ideal geometry) compared to **1**. However, the X-ray studies provided different results than we assumed. Theoretically the clusters of the $[\text{Re}_6(\mu\text{-O})_{12}\text{L}_6]^{n+}$ ($n = 0, 1$) geometry reported here can adopt different site symmetries in the crystal, from 1 (C_1) to $m\bar{3}m$ (O_h). $[\text{Re}_6(\mu\text{-O})_{12}(\text{3-Mepy})_6]\text{BPh}_4$ crystallizes in the form of three kinds of crystals: in $P1$ space group, $[\text{Re}_6(\mu\text{-O})_{12}(\text{3-Mepy})_6]\text{BPh}_4$ (**1a**) and $[\text{Re}_6(\mu\text{-O})_{12}(\text{3-Mepy})_6]\text{BPh}_4\cdot 2(\text{CH}_3\text{CN})$ (**1b**), and in $P2_1/c$ space group, $[\text{Re}_6(\mu\text{-O})_{12}(\text{3-Mepy})_6]\text{BPh}_4\cdot 2(\text{CH}_3\text{CN})$ (**1c**). In **1a–c** crystals the complex cation is located in a general position (C_1 symmetry). In the case of complex **2**, the triclinic crystals comprise the centrosymmetric molecules. As mentioned before, the rhenium atoms in **1a–2** are arranged octahedrally; however, the geometry of the Re_6 core departs from the O_h symmetry (Figure S23, crystal structures, Supporting Information) with the geometrical parameters slightly different from literature values for chalcogenide Re_6 compounds of the $\{\text{Re}_6(\mu_3\text{-Q})_{8-n}(\mu_3\text{-X})_n\}^m$ formula.^{6–9}

The distortions of Re_6 cores from the O_h symmetry were previously described by Baudron and colleagues.¹⁵ In the case of complexes reported here the Re–Re bonds, between adjacent rhenium atoms bridged by O atoms, are in the ranges

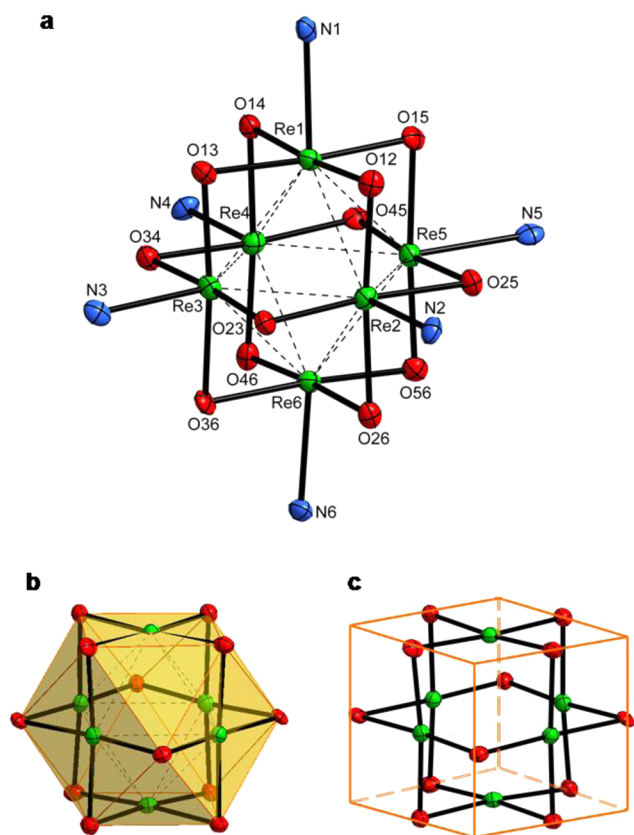


Figure 2. Cube-like geometry of the $[\text{Re}_6(\mu\text{-O})_{12}(\text{3-Mepy})_6]^+$ complex cation of C_1 symmetry (**1a–c**). (a) The $\text{Re}_6(\mu\text{-O})_{12}\text{N}_6$ polyhedron. The aromatic rings are omitted for clarity. (b) Molecular structure of the $\text{Re}_6(\mu\text{-O})_{12}$ unit in the $[\text{Re}_6(\mu\text{-O})_{12}(\text{3-Mepy})_6]\text{BPh}_4$ highlighting the O_{12} -cubo-octahedron encapsulating the Re_6 octahedron. (c) The polyhedron frame built up from the O and Re atoms adopting a topology of a cube without vertices. Color code: Re = green, O = red.

(Table 1) different from those observed in chalcogenide Re_6 complexes,^{6–9} where the typical distance between the nearest neighboring rhenium centers ranges between 2.56 and 2.64 Å. (The discussion for M_6 clusters of such metals as Nb, Ta, W is already known.¹⁶) It is worth mentioning that in studied crystals Re–Re distances nonbridged by O atoms (called trans-[Re-to-Re] distances¹⁵) are very differentiated in the case of **2** compared to **1a–c** (Table 1). Moreover, the asymmetry of Re–($\mu\text{-O}$) bridges and differentiation of Re–O bond lengths in the $\{\text{Re}_6(\mu\text{-O})_{12}\}^{n+}$ ($n = 0, 1$) cores in **1a–2** also contribute to the distortion of oxide rhenium polyhedra from the O_h symmetry (the largest difference between Re–O bond lengths within the bridge is about 0.08 Å in **1b** and 0.27 Å in **2**). The Re–O

bond lengths in **1a–2** are shorter compared to those in Re_6 complexes with one, two, or four $\mu_3\text{-O}$ ligands in the structure.¹⁰ On the whole, despite the differences in geometrical parameters comparing **1** and **2** complexes and deviations of Re_6 polyhedra from O_h symmetry, the overall geometries are the same.

Due to the identical chemical surroundings of each Re atom in **1a–c** crystals and similar geometrical surroundings of each Re atom, we hypothesize that in **1** the unpaired electron density may be delocalized between six Re atoms.

The cyclic voltammetry studies performed for cluster **1** indicated its capabilities to undergo reversible or/and quasireversible reactions, displaying the formation of both reduction and oxidation products. The voltammogram consists of two reduction couples (R1 at –672 mV and R2 at –1829 mV) and one oxidation couple (O1 at 214 mV) (Figure 4). The ΔE_p value for the first reduction wave (R1) equals 61 mV and is assigned to be a reversible one-electron process corresponding to $[\text{Re}_6(\mu\text{-O})_{12}(\text{3-Mepy})_6]\text{BPh}_4$ (**1**)/ $[\text{Re}_6(\mu\text{-O})_{12}(\text{3-Mepy})_6]$ (**2**) redox couple. In the case of R2 and O1 waves the ΔE_p values are about 80 and 74 mV and are attributed to the reversible or quasireversible processes of the rhenium core. Additionally, an anodic peak at 500 mV is observed (Figure S12 in Supporting Information), which suggests the redox process of tetraphenylborate ion.¹⁷

The ^1H NMR and $^{13}\text{C}\{^1\text{H}\}$ NMR spectra performed for **1** and **2** revealed that both cation and molecular complexes adopt approximately O_h symmetry in solution. In spectra all 3-picoline ligands are identical. The ^1H NMR and $^{13}\text{C}\{^1\text{H}\}$ NMR spectra additionally confirm the paramagnetic behavior of **1**. The signals of 3-picoline from complex cation are located out of the expected range. The chemical shifts of *ortho*-H, *para*-H, and *Me*-H protons are upfield whereas the signal of *meta*-H protons is shifted downfield. Additionally, the broad signals of *ortho*-H protons at the ^1H NMR spectrum at 300 K are observed (Figure 5). Decreasing temperature effected high field shifts and broadening of signals of *para*-H (–1.27 ppm at 190 K) and *ortho*-H protons (–3.28, –3.64 ppm at 190 K) as well as upfield shift of the *Me*-H protons signal (–0.80 ppm at 190 K) (Figure 5) and downfield shift of signal of the *meta*-H protons (10.36 ppm at 190 K). The temperature dependences of the chemical shifts indicate the dominant contact contribution to the isotropic shifts (Supporting Information Figure S3). Besides, the observed alternation of signs of chemical shifts is indicative of π -delocalization of spin density.¹⁸ In the case of **2** the chemical shifts at the ^1H and $^{13}\text{C}\{^1\text{H}\}$ NMR spectra collected for **2** are expected for diamagnetic species.

In addition to **1** and **2** complexes, we obtained a lot of other crystalline clusters from ReX_3 ($X = \text{Cl, Br, I}$), which belong to the new $\text{Re}_6(\mu\text{-O})_{12}\text{L}_6$ class of rhenium complexes of symmetry

Table 1. Ranges of Selected Interatomic Distances (Å) and Angles (deg) for **1a–2** Crystals

	$[\text{Re}_6(\mu\text{-O})_{12}(\text{3-Mepy})_6]\text{BPh}_4$ (1)			$[\text{Re}_6(\mu\text{-O})_{12}(\text{3-Mepy})_6]$ (2)
	1a	1b	1c	
Re–Re bonds	2.5909(12)–2.7480(10)	2.6256(12)–2.7181(14)	2.6006(6)–2.7532(7)	2.5804(8)–2.8766(13)
av Re–Re bond	2.6634(11)	2.6621(13)	2.6649(8)	2.6786(11)
Re...Re distances (spatial diagonals in Re_6 polyhedra)	3.7493(12)–3.7841(12)	3.7424(13)–3.7798(16)	3.7508(10)–3.7888(11)	3.6377(14)–3.8709(15)
Re–O bonds	1.922(3)–1.971(3)	1.906(9)–1.975(8)	1.927(4)–1.977(4)	1.848(5)–2.119(5)
Re–O–Re angles	83.87(13)–89.71(15)	84.3(4)–88.2(3)	84.52(15)–89.22(15)	82.07(18)–92.30(13)
Re–N bonds	2.144(4)–2.175(4)	2.143(10)–2.184(11)	2.146(4)–2.176(5)	2.156(6)–2.164(5)

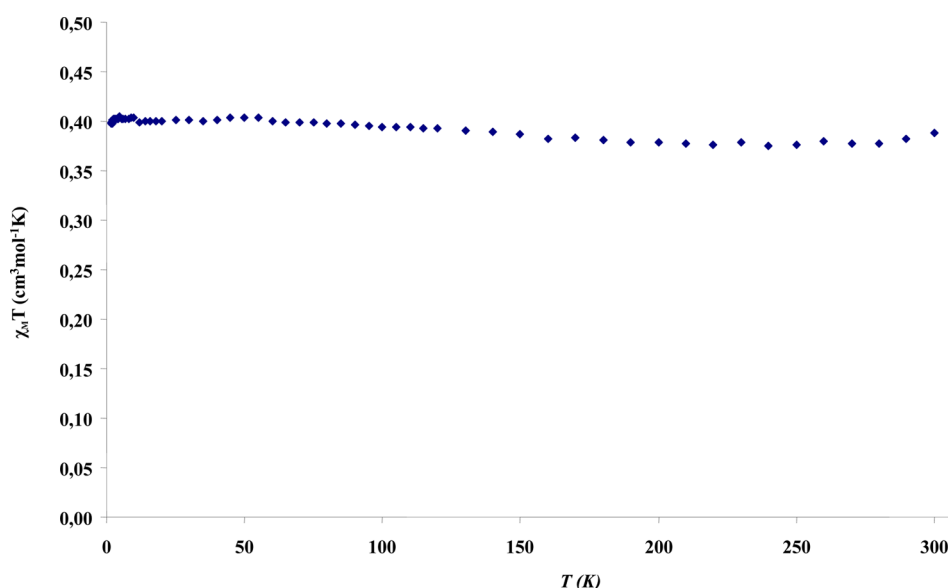


Figure 3. Temperature dependence of magnetic susceptibility of 1 compound (1.7–300 K, 0.5 T).

Table 2. Selected Crystal Data and Structure Refinement Parameters of 1a–2 crystals

	1a	1b	1c	2
Crystal Data				
empirical formula	$[\text{Re}_6(\mu\text{-O})_{12}(\text{3-Mepy})_6]\text{BPh}_4$	$[\text{Re}_6(\mu\text{-O})_{12}(\text{3-Mepy})_6]\text{BPh}_4 \cdot 2(\text{CH}_3\text{CN})$	$[\text{Re}_6(\mu\text{-O})_{12}(\text{3-Mepy})_6]\text{BPh}_4 \cdot 2(\text{CH}_3\text{CN})$	$[\text{Re}_6(\mu\text{-O})_{12}(\text{3-Mepy})_6] \cdot 11(\text{H}_2\text{O})$
fw (g mol ⁻¹)	2187.17	2269.27	2269.27	2066.13
cryst syst, space group	triclinic, $P\bar{1}$	triclinic, $P\bar{1}$	monoclinic, $P2_1/c$	triclinic, $P\bar{1}$
<i>a</i> (Å)	11.123(3)	10.475(3)	10.843(3)	10.369(3)
<i>b</i> (Å)	17.492(5)	18.116(6)	26.996(7)	10.409(3)
<i>c</i> (Å)	17.919(5)	18.230(6)	22.527(6)	13.138(4)
α (deg)	61.55(3)	77.45(3)		104.98(3)
β (deg)	78.63(3)	78.09(3)	90.66(3)	96.37(3)
γ (deg)	88.77(3)	79.70(3)		105.83(3)
<i>V</i> (Å ³)	2995(2)	3271(2)	6594(3)	1292(7)
<i>Z</i>	2	2	4	1
μ (mm ⁻¹)	12.14	11.12	11.04	14.08
<i>F</i> (000)	2030	2118	4236	956
cryst size (mm ³)	0.36 × 0.04 × 0.03	0.16 × 0.03 × 0.02	0.21 × 0.08 × 0.06	0.10 × 0.08 × 0.07
cryst color	brown	orange	red	red
crystal form	needle	plate	block	block
Data Collection				
diffractometer	Xcalibur with CCD onyx detector	Xcalibur with CCD ruby detector	Kuma KM-4-CCD	Xcalibur with CCD ruby detector
radiation type, wavelength, λ (Å)	Mo <i>K</i> α , 0.710 73	Mo <i>K</i> α , 0.710 73	Mo <i>K</i> α , 0.710 73	Mo <i>K</i> α , 0.710 73
<i>T</i> (K)	100(2)	100(2)	100(2)	110(2)
Θ range (deg)	2.44–38.47	2.71–28.75	2.89–36.87	2.88–31.00
<i>h</i> , <i>k</i> , <i>l</i> range	–14 ≤ <i>h</i> ≤ 12 –23 ≤ <i>k</i> ≤ 23 –23 ≤ <i>l</i> ≤ 23	–14 ≤ <i>h</i> ≤ 12 –23 ≤ <i>k</i> ≤ 22 –23 ≤ <i>l</i> ≤ 24	–14 ≤ <i>h</i> ≤ 15 –32 ≤ <i>k</i> ≤ 37 –31 ≤ <i>l</i> ≤ 31	–10 ≤ <i>h</i> ≤ 13 –16 ≤ <i>k</i> ≤ 16 –31 ≤ <i>l</i> ≤ 31
measured reflns	30 305	24 939	85 263	12 748
indep reflns	14 130	14 684	19 042	5640
obsd reflns (<i>I</i> > 2 σ (<i>I</i>))	9489	8484	10 514	4919
<i>R</i> _{int}	0.033	0.056	0.085	0.032
Refinement				
refinement on	<i>F</i> ²	<i>F</i> ²	<i>F</i> ²	<i>F</i> ²
data/restraints/params	14 130/0/772	14 684/53/801	19 042/0/828	5640/0/338
<i>R</i> [<i>F</i> ² > 2 σ (<i>F</i> ²)]	0.025	0.065	0.037	0.031
<i>wR</i> (<i>F</i> ²)	0.04	0.098	0.042	0.073
GOF = <i>S</i>	1.00	1.03	0.98	1.14
$\Delta\rho_{\text{max}}/\Delta\rho_{\text{min}}$ (e Å ⁻³)	1.71/–1.23	2.06/–1.82	2.56/–1.62	3.20/–1.11

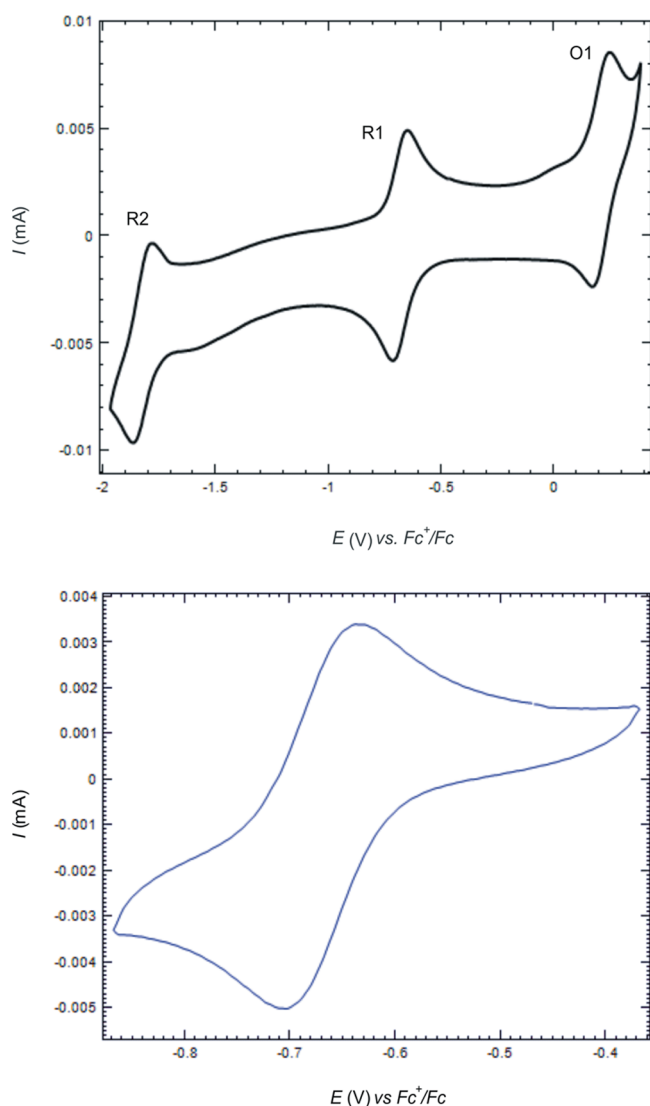


Figure 4. Cyclic voltammograms of **1** showing redox couples. Top: CV in the range -2000 – 400 mV, displaying three waves: (R1) at -672 mV, (R2) at -1829 mV, (O1) at 214 mV versus Fc^+/Fc couple in MeCN in the presence of $(\text{NBu}_4)[\text{PF}_6]$. Bottom: CV showing the reversible $[\text{Re}_6(\mu\text{-O})_{12}(\text{3-Mepy})_6]^+ / [\text{Re}_6(\mu\text{-O})_{12}(\text{3-Mepy})_6]$ redox couple (R1). (Scan rate = 0.1 V/s).

ranging from 1 (C_1) to $m\bar{3}m$ (O_h) and different degrees of ionization, which will be published in the near future.

CONCLUSIONS

In summary, we synthesized the first cube-like $[\text{Re}_6(\mu\text{-O})_{12}(\text{3-Mepy})_6]\text{BPh}_4$ (**1**) and $[\text{Re}_6(\mu\text{-O})_{12}(\text{3-Mepy})_6]$ (**2**) complexes, which establish a new class of hexanuclear metal clusters. They are the first that consist of the unique $\{\text{Re}_6(\mu\text{-O})_{12}\}^n$ ($n = 0, 1$) core built up from octahedrally arranged Re atoms inscribed within an O_{12} -cubo-octahedron. We created a novel strategy for the syntheses of polynuclear rhenium complexes, based on facile and short-term one-pot reaction between rhenium(III) halides and aromatic amines in the presence of water.

The cyclic voltammetry experiments unambiguously indicated that **1** complex can be reduced and oxidized in a reversible or/and quasireversible mode. We successfully chemically reduced **1**, which led to the formation of the molecular complex **2** as member of a

redox couple $[\text{Re}_6(\mu\text{-O})_{12}(\text{3-Mepy})_6]^+ / [\text{Re}_6(\mu\text{-O})_{12}(\text{3-Mepy})_6]$ (**2**). These results show that changing of oxidation states of rhenium atoms in the cluster **1** proceeded without an alternation of the overall molecular geometry of the complex.

EXPERIMENTAL SECTION

Procedures. Rhenium(III) iodide used for syntheses was synthesized and purified according to the procedure published by Malatesta.¹⁹ The 3-picoline was purchased from Sigma-Aldrich Co. and was purified by distillation over CaH_2 under dinitrogen before use. Distilled water was degassed before use. Reaction was carried out under dinitrogen.

Synthesis of $[\text{Re}_6(\mu\text{-O})_{12}(\text{3-Mepy})_6]\text{BPh}_4$ (1**).** The rhenium(III) iodide (2.05 g, 3.61 mmol) was mixed with water (2.00 mL, 111 mmol), and 3-methylpyridine (10.0 mL) was added. The mixture was heated at 45 °C with constant stirring for ca. 10 min, and then the stirring was continuing for ca. 30 min without heating. After that the mixture was washed several times with hexane and left under dinitrogen to evaporate the residue of 3-picoline. Then, the crude product was dissolved in acetonitrile and left in the refrigerator. After several hours the fine crystalline product was obtained which then was filtered off, washed quickly with acetone (ca. 10 mL), and dissolved in the solution of NaBPh_4 (ca. 0.44 g, 1.3 mmol) in acetonitrile (ca. 300 mL) and left for crystallization under gentle stream of dinitrogen. The mixture of brownish red crystals in the form of needle-like plates and needle-like blocks of $[\text{Re}_6\text{O}_{12}(\text{3-Mepy})_6]\text{BPh}_4$ (**1**) appeared. Three kinds of crystals were obtained: $[\text{Re}_6\text{O}_{12}(\text{3-Mepy})_6]\text{BPh}_4$ (**1a**) and polymorphs $[\text{Re}_6\text{O}_{12}(\text{3-Mepy})_6]\text{BPh}_4 \cdot 2(\text{CH}_3\text{CN})$ (**1b**, **1c**). Data presented below were collected after removing acetonitrile from all crystals under vacuum. Yield: 0.369 g, 169 mmol, 28% . Anal. Calcd for $\text{C}_{60}\text{H}_{62}\text{BN}_6\text{O}_{12}\text{Re}_6$ (2187.24 g/mol): C, 32.95 ; H, 2.86 ; N, 3.84 . Found: C, 33.31 ; H, 2.91 ; N, 3.72% . ICP Anal. Calcd: Re, 51.08 . Found: Re, 50.72% . ESI-MS (CH_3CN): $m/z = 1868.0179$ [M^+] (calcd for $[\text{Re}_6(\mu\text{-O})_{12}(\text{3-Mepy})_6]^+$ 1868.0147), $m/z = 319.1862$ (calcd for BPh_4^- 319.2271). ^1H NMR (500 MHz, CD_2Cl_2 , 25 °C) δ 9.29 ppm (m, $^3J = 5.0$ Hz, 6H , $\text{H}_{\text{meta}(m2)}$), 7.32 ppm (m, 8H , H_{ortho} from BPh_4^- ion), 7.03 ppm (t, 8H , H_{meta} in BPh_4^-), 6.87 ppm (t, 4H , H_{para} from BPh_4^-), 2.53 ppm (m, $^3J = 5.0$ Hz, 6H , $\text{H}_{\text{para}(p)}$), 2.04 ppm (m, 6H , $\text{H}_{\text{ortho}(o1)}$), 1.90 ppm (m, 6H , $\text{H}_{\text{ortho}(o2)}$), 0.58 ppm (s, 18H , H_{Me}). $^{13}\text{C}\{^1\text{H}\}$ NMR (125 MHz, CD_2Cl_2 , 25 °C) δ 235.37 ppm ($\text{C}_{\text{ortho}(o2)}$), 232.34 ppm ($\text{C}_{\text{ortho}(o1)}$), 172.47 ppm ($\text{C}_{\text{para}(p)}$), 164.63 ppm (BPh_4^-), 136.43 ppm (BPh_4^-), 126.28 ppm (BPh_4^-), 122.34 ppm (BPh_4^-), 112.63 ppm ($\text{C}_{\text{meta}(m1)}$), 100.33 ppm ($\text{C}_{\text{meta}(m2)}$), 23.05 ppm (C_{Me}) (Supporting Information Figure S3). IR (KBr, cm^{-1}): 705 $\nu(\text{Re}-(\mu\text{-O}))$. FIR (nujol, cm^{-1}): 524 $\delta(\text{Re}-(\mu\text{-O}))$, 303 $\gamma(\text{Re}-(\mu\text{-O}))$.

Synthesis of $[\text{Re}_6(\mu\text{-O})_{12}(\text{3-Mepy})_6] \cdot 11(\text{H}_2\text{O})$ (2**).** Complex **1** (25.00 mg, 11.43 μmol) was dissolved in ca. 10 mL of acetonitrile and treated with the 80% solution of hydrazine hydrate (111.2 μL , 2.858 μmol). The fine-crystalline brown-violet crude product was obtained which was filtered off and recrystallized from water resulting in the formation of dark red crystals of complex **2** in near quantitative yield. The same result was achieved in the course of recrystallization from methanol.

Anal. Calcd for $\text{C}_{36}\text{H}_{42}\text{N}_6\text{O}_{12}\text{Re}_6$ (1868.00 g/mol): C, 23.15 ; H, 2.27 ; N, 4.50 . Found: C, 22.78 ; H, 2.31 ; N, 4.25% . ESI-MS (CH_3CN): $m/z = 1868.0827$ [M^+] (calcd for $[\text{Re}_6(\mu\text{-O})_{12}(\text{3-Mepy})_6]^+$ 1868.0147). ^1H NMR (500 MHz, D_2O , 300 K) δ 9.09 ppm (m, 6H , $\text{H}_{\text{ortho}(o1)}$), 9.04 ppm (m, $^3J = 5.5$ Hz, 6H , $\text{H}_{\text{ortho}(o2)}$), 8.05 ppm (d, $^3J = 7.5$ Hz, 6H , $\text{H}_{\text{para}(p)}$), 7.77 ppm (t, $^3J = 7.5$ Hz, 6H , $\text{H}_{\text{meta}(m2)}$), 2.46 ppm (s, 18H , H_{Me}). $^{13}\text{C}\{^1\text{H}\}$ NMR (125 MHz, D_2O , 300 K; chemical shifts were referenced to MeOH used as an internal standard (δ 49.50 ppm (C_{MeOH})) δ 154.81 ppm ($\text{C}_{\text{ortho}(o1)}$), 151.88 ppm ($\text{C}_{\text{ortho}(o2)}$), 142.65 ppm ($\text{C}_{\text{para}(p)}$), 137.53 ppm ($\text{C}_{\text{meta}(m1)}$), 126.14 ppm ($\text{C}_{\text{meta}(m2)}$), 17.72 ppm (C_{Me}) (Supporting Information Figures S13 and S14). IR (KBr, cm^{-1}): 701 , 681 $\nu(\text{Re}-(\mu\text{-O}))$. FIR (nujol, cm^{-1}): 510 $\delta(\text{Re}-(\mu\text{-O}))$, 313 $\gamma(\text{Re}-(\mu\text{-O}))$. Crystal data are available in Table 2.

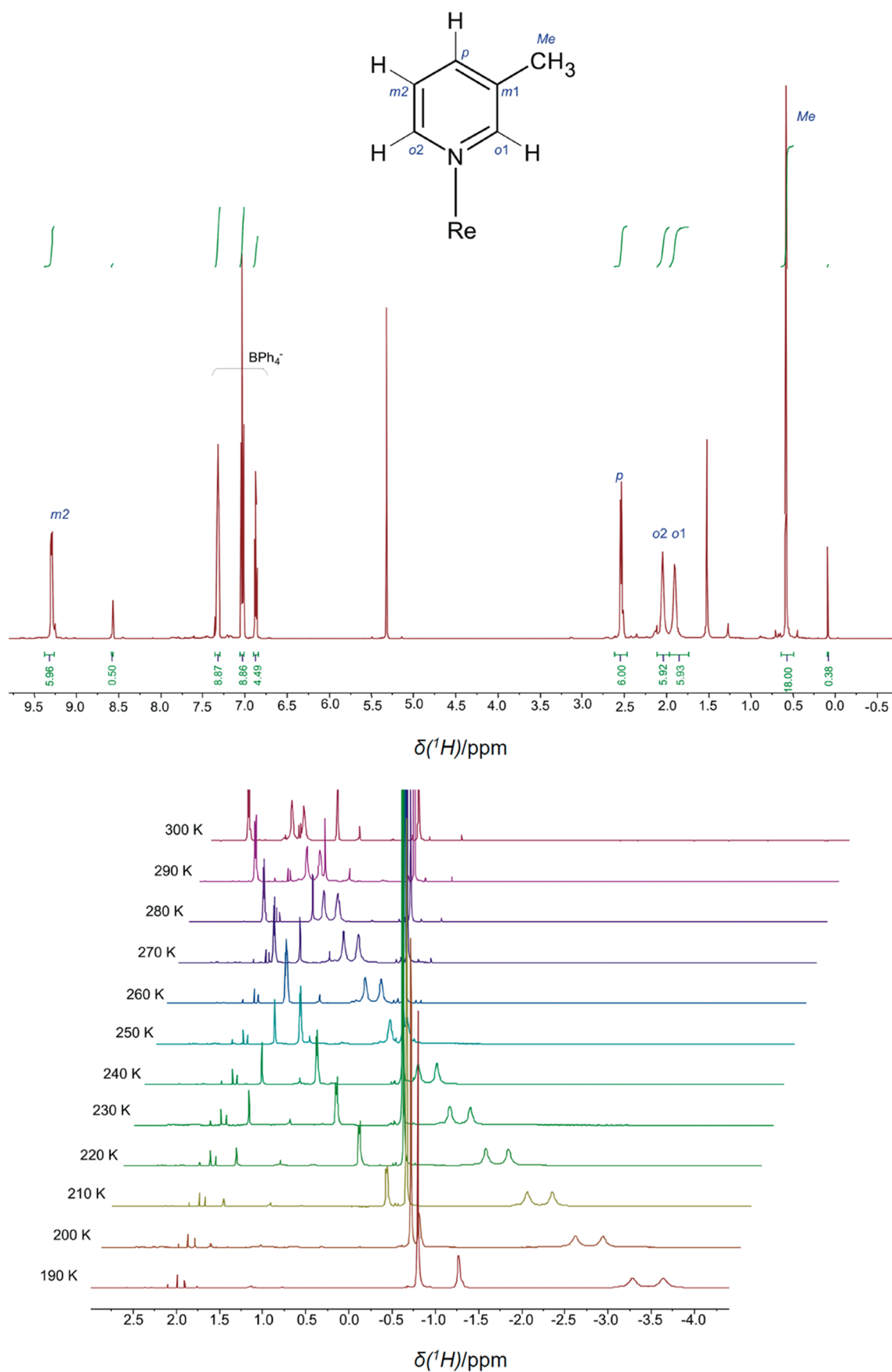


Figure 5. ^1H NMR spectrum of complex 1 (500 MHz, CD_2Cl_2 , 300 K) (top) and temperature dependence of ^1H chemical shifts for 1 (500 MHz, CD_2Cl_2 , 190–300 K) (bottom). Excessive integrations of signals derived from BPh_4^- ion result from a presence of traces of NaBPh_4 (used in reaction of 1) on the surface of crystals taken for measurements.

■ ASSOCIATED CONTENT

■ Supporting Information

^1H and $^{13}\text{C}\{^1\text{H}\}$ NMR spectra for **1** and **2**; COSY, HMQC spectra and temperature dependence of ^1H chemical shifts for **1**; X-ray crystallographic data in CIF format for **1a–2**; selected crystal data and structure refinement parameters, temperature dependence of magnetic susceptibility, IR, FIR, ESI-MS mass spectra, descriptions of crystal structure and distortion of Re_6 polyhedrons in **1a–2**. This material is available free of charge via the Internet at <http://pubs.acs.org>. The crystallographic data have been deposited at the Cambridge Crystallographic Data Centre and were assigned the deposition numbers CCDC 959650–959653.

■ AUTHOR INFORMATION

Corresponding Author

*E-mail: marta.krawczyk@chem.uni.wroc.pl, martakrawczyk.re@gmail.com.

Notes

The authors declare no competing financial interest.

■ ACKNOWLEDGMENTS

Financial support from the National Science Center (Grant NCN UMO-2011/03/N/ST5/04844) is gratefully acknowledged.

■ REFERENCES

- (1) See for example: (a) Xiao, F.; Hao, J.; Zhang, J.; Lv, C.; Yin, P.; Wang, L.; Wei, Y. *J. Am. Chem. Soc.* **2010**, *132*, 5956–5957. (b) Maguerès, P. Le.; Hubig, S. M.; Lindeman, S. V.; Veya, P.; Kochi, J. K. *J. Am. Chem. Soc.* **2000**, *122*, 10073–10082. (c) Xu, H.; Li, Z.; Liu, B.; Xue, G.; Hu, H.; Fu, F.; Wang, J. *Cryst. Growth Des.* **2010**, *10*, 1096–1103. (d) Errington, R. J.; Petkar, S. S.; Middleton, P. S.; McFarlane, W.; Clegg, W.; Coxall, R. A.; Harrington, R. W. *J. Am. Chem. Soc.* **2007**, *129*, 12181–12196. (e) Ohlin, C. A.; Villa, E. M.; Fettingler, J. C.; Casey, W. H. *Angew. Chem., Int. Ed.* **2008**, *47*, 8251–8254. (f) Niu, J.; Fu, X.; Zhao, J.; Li, S.; Ma, P.; Wang, J. *Cryst. Growth Des.* **2010**, *10*, 3110–3119.
- (2) (a) Hibble, S. J.; McGrellis, S. A. *J. Chem. Soc., Dalton Trans.* **1995**, 1947–1949. (b) Anokhina, E. V.; Essig, M. W.; Day, C. S.; Lachgar, A. *J. Am. Chem. Soc.* **1999**, *121*, 6827–6833. (c) Dronskowski, R.; Simon, A. *Angew. Chem.* **1989**, *101*, 775–776. (d) Dronskowski, R.; Simon, A. *Acta Chem. Scand.* **1991**, *45*, 850–855. (e) Lindblom, B.; Strandberg, R. *Acta Chem. Scand.* **1989**, *43*, 825–828. (f) Hibble, S. J.; Cooper, S. P.; Hannon, A. C.; Patat, S.; McCarroll, W. H. *Inorg. Chem.* **1998**, *37*, 6839–6846. (g) Hibble, S. J.; Cooper, S. P.; Patat, S.; Hannon, A. C. *Acta Crystallogr., Sect. B* **1999**, *55*, 683–697.
- (3) (a) Roland, B. K.; Flora, W. H.; Selby, H. D.; Armstrong, N. R.; Zheng, Z. *J. Am. Chem. Soc.* **2006**, *128*, 6620–6625. (b) Selby, H. D.; Roland, B. K.; Flora, W. H.; Armstrong, N. R.; Zheng, Z. *C. R. Chim.* **2005**, *8*, 1798–1807. (d) Molard, Y.; Dorson, F.; Brylew, K. A.; Shestopalov, M. A.; Gal, Y. L.; Cordier, S.; Mironov, Y. V.; Kitamura, N.; Perrin, C. *Chem.—Eur. J.* **2010**, *16*, 5613–5619. (e) Molard, Y.; Ledneva, A.; Amela-Cortes, M.; Circo, V.; Naumov, N. G.; Mériadec, C.; Artzner, F.; Cordier, S. *Chem. Mater.* **2011**, *23*, 5122–5130. (f) Shestopalov, M. A.; Cordier, S.; Hernandez, O.; Molard, Y.; Perrin, C.; Perrin, A.; Fedorov, V. E.; Mironov, Y. V. *Inorg. Chem.* **2009**, *48*, 1482–1489.
- (4) (a) Gray, T. G.; Rudzinski, C. M.; Meyer, E. E.; Holm, R. H.; Nocera, D. G. *J. Am. Chem. Soc.* **2003**, *125*, 4755–4770. (b) Arratia-Pérez, R.; Hernández-Acevedo, L. *J. Chem. Phys.* **1999**, *111*, 168–172. (c) Cordier, S.; Fabre, B.; Molard, Y.; Fadjie-Djomkam, A.-B.; Tournerie, N.; Ledneva, A.; Naumov, N. G.; Moreac, A.; Turban, P.; Tricot, S.; Ababou-Girard, S.; Godet, C. *J. Phys. Chem. C* **2010**, *114*, 18622–18633. (d) Aubert, T.; Ledneva, A. Y.; Grasset, F.; Kimoto, K.

Naumov, N. G.; Molard, Y.; Saito, N.; Haneda, H.; Cordier, S. *Langmuir* **2010**, *26*, 18512–18518.

(5) Durham, J. L.; Tirado, J. N.; Knott, S. A.; Oh, M. K.; McDonald, R.; Szczepura, L. F. *Inorg. Chem.* **2012**, *51*, 7825–7836.

(6) (a) Opalovskii, A. A.; Fedorov, V. E.; Lobkov, E. U. *Zh. Neorg. Khim.* **1971**, *16*, 1494–1496. (b) Opalovskii, A. A.; Fedorov, V. E.; Lobkov, E. U.; Erenburg, B. G. *Zh. Neorg. Khim.* **1971**, *16*, 3175–3177. (7) Gray, T. G. *Coord. Chem. Rev.* **2003**, *243*, 213–235.

(8) Cambridge Structural Database (CSD, August 2012 release, Version 5.32): Allen, F. H. *Acta Crystallogr., Sect. B* **2002**, *B58*, 380–388.

(9) Knott, S. A.; Templeton, J. N.; Durham, J. L.; Howard, A. M.; McDonald, R.; Szczepura, L. F. *Dalton Trans.* **2013**, *42*, 8132–8139.

(10) (a) Yaghi, O. M.; Scott, M. J.; Holm, R. H. *Inorg. Chem.* **1992**, *31*, 4778–4784. (b) Decker, A.; Simon, F.; Boubekeur, K.; Fenske, D.; Batail, P. Z. *Anorg. Allg. Chem.* **2000**, *626*, 309–313. (c) Uriel, S.; Boubekeur, K.; Batail, P.; Orduna, J.; Canadell, E. *Inorg. Chem.* **1995**, *34*, 5307–5313. (d) Deluzet, A.; Rousseau, R.; Guilbaud, C.; Granger, I.; Boubekeur, K.; Batail, P.; Canadell, E.; Auban-Senzier, P.; Jérôme, D. *Chem.—Eur. J.* **2002**, *8*, 3884–3900. (e) Mironov, Y. V.; Shestopalov, M. A.; Brylew, K. A.; Yarovoi, S. S.; Romanenko, G. V.; Fedorov, V. E.; Spies, H.; Pietzsch, H.-J.; Stephan, H.; Geipel, G.; Bernhard, G.; Kraus, W. *Eur. J. Inorg. Chem.* **2005**, 657–661. (f) Simon, F.; Boubekeur, K.; Gabriel, J.-C. P.; Batail, P. *Chem. Commun.* **1998**, 845–846. (g) Yarovoi, S. S.; Mironov, Y. V.; Solodovnikov, S. F.; Naumov, D. Y.; Moroz, N. K.; Kozlova, S. G.; Simon, A.; Fedorov, V. E. *Chem. Commun.* **2005**, 719–721.

(11) (a) Koz'min, P. A.; Kotelnikova, A. S.; Larina, T. B.; Mekhtiev, M. M.; Surazhskaya, M. D.; Bagirov, S. A.; Osmanov, N. S. *Dokl. Akad. Nauk SSSR* **1987**, *295*, 647. (b) Koz'min, P. A.; Osmanov, N. S.; Larina, T. B.; Kotelnikova, A. S.; Surazhskaya, M. D.; Abbasova, T. A. *Dokl. Akad. Nauk SSSR* **1989**, *306*, 378–381.

(12) Schäfer, H.; Schnering, H. G. *Angew. Chem.* **1964**, *76*, 833–849.

(13) Bennett, M. J.; Cotton, F. A.; Foxman, B. M. *Inorg. Chem.* **1968**, *7*, 1563–1569.

(14) Agilent. *CrysAlis PRO*; Agilent Technologies: Yarnton, U. K., 2011.

(15) Baudron, S. A.; Deluzet, A.; Boubekeur, K.; Batail, P. *Chem. Commun.* **2002**, 2124–2125.

(16) (a) Oligaro, F.; Cordier, S.; Halet, J.-F.; Perrin, C.; Saillard, J.-Y.; Sergent, M. *Inorg. Chem.* **1998**, 6199–6207. (b) Fontaine, B.; Cordier, S.; Gautier, R.; Gulo, F.; Halet, J.-F.; Perić, B.; Perrin, P. *New J. Chem.* **2011**, *35*, 2245–2252. (c) Nebbache, N.; Fontaine, B.; Meyer, H.-J.; Gautier, R.; Halet, J.-F. *Solid State Sci.* **2013**, *150*–155. (d) Tragl, S.; Ströbele, M.; Glaser, J.; Vicent, C.; Llusar, R.; Meyer, H.-J. *Inorg. Chem.* **2009**, *48*, 3825–3831.

(17) Pal, P. K.; Chowdhury, S.; Drew, M. G. B.; Datta, D. *New J. Chem.* **2002**, *26*, 367–371.

(18) (a) Bertini, I.; Luchinat, C.; Parigi, G. *Solution NMR of Paramagnetic Molecules. Applications to Metallobiomolecules and Models*; Elsevier Science: Amsterdam, 2001; pp 28–51. (b) La Mar, G. N.; Eaton, G. R.; Holm, R. H.; Walker, F. A. *J. Am. Chem. Soc.* **1973**, *95*, 63–75. (c) Chmielewski, P. J.; Latos-Grażyński, L.; Rachlewicz, K. *Magn. Reson. Chem.* **1993**, *31*, S47–S52.

(19) Malatesta, L. *Inorg. Synth.* **1963**, *7*, 185–189.